

First measurement of massive virtual photon emission from N* baryon resonances

R. Abou Yassine^{6,13}, J. Adamczewski-Musch⁵, O. Arnold^{10,9}, E.T. Atomssa¹³, M. Becker¹¹, C. Behnke⁸, J.C. Berger-Chen^{10,9}, A. Blanco¹, C. Blume^{8,5,e}, M. Böhmer¹⁰, L. Chlad^{14,g}, P. Chudoba^{14,g}, I. Ciepał³, S. Deb¹³, C. Deveaux¹¹, D. Dittert⁶, J. Dreyer⁷, E. Epple^{10,9}, L. Fabbietti¹⁰, P. Fonte^{1,a}, C. Franco¹, J. Friese¹⁰, I. Fröhlich⁸, J. Fortsch¹⁸, T. Galatyuk^{6,5,c}, J. A. Garzón¹⁵, R. Gernhäuser¹⁰, R. Greifehagen^{7,d}, M. Grunwald¹⁷, M. Gumberidze⁵, S. Harabasz^{6,c}, T. Heinz⁵, T. Hennino¹³, C. Höhne^{11,5}, F. Hojeij¹³, R. Holzmann⁵, M. Idzik², B. Kämpfer^{7,d}, K-H. Kampert¹⁸, B. Kardan^{8,e}, V. Kedych⁶, I. Koenig⁵, W. Koenig⁵, M. Kohls^{8,e}, J. Kolas¹⁷, B. W. Kolb⁵, G. Korcyl⁴, G. Kornakov¹⁷, R. Kotte⁷, W. Krueger⁶, A. Kugler¹⁴, T. Kunz¹⁰, R. Lalik⁴, K. Lapidus^{10,9}, S. Linev⁵, F. Linz^{6,5}, L. Lopes¹, M. Lorenz⁸, T. Mahmoud¹¹, L. Maier¹⁰, A. Malige⁴, J. Markert⁵, S. Maurus¹⁰, V. Metag¹¹, J. Michel⁸, D.M. Mihaylov^{10,9}, V. Mikhaylov^{14,g}, A. Molenda², C. Müntz⁸, R. Münzer^{10,9}, M. Nabroth⁸, L. Naumann⁷, K. Nowakowski⁴, J. Orliński¹⁶, J.-H. Otto¹¹, Y. Parpottas¹², M. Parschau⁸, C. Pauly¹⁸, V. Pechenov⁵, O. Pechenova⁵, K. Piasecki¹⁶, J. Pietraszko⁵, T. Povar¹⁸, K. Prościński^{4,b}, A. Prozorov^{14,f}, W. Przygoda⁴, K. Pysz³, B. Ramstein¹³, N. Rathod¹⁷, P. Rodriguez-Ramos^{14,g}, A. Rost^{6,5}, A. Rustamov⁵, P. Salabura⁴, T. Scheib⁸, N. Schild⁶, K. Schmidt-Sommerfeld¹⁰, H. Schuldes⁸, E. Schwab⁵, F. Scozzi^{6,13}, F. Seck⁶, P. Sellheim⁸, J. Siebenson¹⁰, L. Silva¹, U. Singh⁴, J. Smyrski⁴, S. Spataro^h, S. Spies⁸, M. Stefaniak⁵, H. Ströbele⁸, J. Stroth^{8,5,e}, C. Sturm⁵, K. Sumara⁴, O. Svoboda¹⁴, M. Szala⁸, P. Tlusty¹⁴, M. Traxler⁵, H. Tsertos¹², I. C. Udea^{6,5}, O. Vazquez-Doce^{10,9}, V. Wagner¹⁴, A.A. Weber¹¹, C. Wendisch⁵, M.G. Wiebusch⁵, J. Wirth^{10,9}, A. Władyszewska^{4,b}, H.P. Zbroszczyk¹⁷, E. Zherebtsova^{5,i}, M. Zieliński⁴, P. Zumbach⁵

(HADES collaboration)

¹LIP-Laboratório de Instrumentação e Física Experimental de Partículas , 3004-516 Coimbra, Portugal

²AGH University of Krakow, Faculty of Physics and Applied Computer Science, 30-059 Krakow, Poland

³Institute of Nuclear Physics, Polish Academy of Sciences, 31342 Kraków, Poland

⁴Smoluchowski Institute of Physics, Jagiellonian University of Cracow, 30-059 Kraków, Poland

⁵GSI Helmholtzzentrum für Schwerionenforschung GmbH, 64291 Darmstadt, Germany

⁶Institut für Kernphysik, Technische Universität Darmstadt, 64289 Darmstadt, Germany

⁷Institut für Strahlenphysik, Helmholtz-Zentrum Dresden-Rossendorf, 01314 Dresden, Germany

⁸Institut für Kernphysik, Goethe-Universität, 60438 Frankfurt, Germany

⁹Excellence Cluster 'Origin and Structure of the Universe', 85748 Garching, Germany

¹⁰Physik Department E62, Technische Universität München, 85748 Garching, Germany

¹¹II.Physikalisches Institut, Justus Liebig Universität Giessen, 35392 Giessen, Germany

¹²Department of Mechanical Engineering, Frederick University, 1036 Nicosia, Cyprus

¹³Laboratoire de Physique des 2 infinis Irene Joliot-Curie, Université Paris-Saclay, CNRS-IN2P3. , F-91405 Orsay , France

¹⁴Nuclear Physics Institute, The Czech Academy of Sciences, 25068 Rez, Czech Republic

¹⁵LabCAF. F. Física, Univ. de Santiago de Compostela, 15706 Santiago de Compostela, Spain

¹⁶Uniwersytet Warszawski - Instytut Fizyki Doświadczalnej, 02-093 Warszawa, Poland

¹⁷Warsaw University of Technology; Faculty of Physics, 00-662 Warsaw, Poland

¹⁸Bergische Universität Wuppertal, 42119 Wuppertal, Germany

^a also at Instituto Politecnico de Coimbra, Instituto Superior de Engenharia de Coimbra, 3030-199 Coimbra, Portugal

^b also at Doctoral School of Exact and Natural Sciences, Jagiellonian University, Cracow, Poland

^c also at Helmholtz Research Academy Hesse for FAIR (HFHF), Campus Darmstadt, 64390 Darmstadt, Germany

^d also at Technische Universität Dresden, 01062 Dresden, Germany

^e also at Helmholtz Research Academy Hesse for FAIR (HFHF), Campus Frankfurt , 60438 Frankfurt am Main, Germany

^f also at Charles University, Faculty of Mathematics and Physics, 12116 Prague, Czech Republic

^g also at Czech Technical University in Prague, 16000 Prague, Czech Republic

^h also at Dipartimento di Fisica and INFN, Università di Torino, 10125 Torino, Italy

ⁱ also at University of Wrocław, 50-204 Wrocław, Poland

and

M. Zetenyi^j

^j Wigner Research Centre for Physics, Budapest, Hungary.

First information on the time-like electromagnetic structure of baryons in the second resonance region has been obtained from measurements of dielectron (e^+e^-) invariant mass and angular distributions in the quasi-free reaction $\pi^-p \rightarrow n e^+e^-$ at $\sqrt{s_{\pi p}} = 1.49$ GeV with the High Acceptance Di-Electron Spectrometer (HADES) at GSI using the pion beam impinging on a CH₂ target. We find a total cross section $\sigma = 2.97 \pm 0.07^{\text{data}} \pm 0.21^{\text{acc}} \pm 0.31^{\text{Zeff}} \mu\text{b}$. In complement to the

analysis of the inclusive e^+e^- channel, this data set provides a crucial test of the description of baryon time-like transitions. Approaches based on a Vector Meson Dominance amplitude containing direct photon and vector meson (ρ) couplings to the baryon provide a satisfactory agreement with the data. A good description is also obtained by electromagnetic time-like baryon transition form factors in a covariant spectator-quark model, pointing to the dominance of meson cloud effects. The dielectron angular distributions exhibit the contributions of virtual photons (γ^*) with longitudinal polarization, in contrast to real photons. The virtual photon angular dependence supports the dominance of $J=3/2$, $I=1/2$ contributions observed in both the γ^*n and the $\pi\pi n$ channels.

Introduction. Hadrons are composite quantum objects, characterized by a number of parameters, such as mass, charge, spin or form factors, which derive from the strong-interaction. However, despite the impressive progress made by first-principle approaches, concerted actions of theory and experiment are still needed before they can be inferred directly from Quantum Chromodynamics (QCD). This motivates, in particular, the extensive studies of electromagnetic Transition Form Factors (eTFF) for the transition between a nucleon (N) and baryon resonances (R) ($N\gamma^* \rightarrow R$) with electron scattering. In such experiments the squared four-momentum q^2 of the virtual photon (γ^*) is negative, probing the form factors in the space-like region [1–5]. However, a consistent understanding of baryon electromagnetic structure also requires experimental information in the time-like region $q^2 > 0$ which is very scarce [6–8]. eTFF, which encode the electromagnetic structure of involved baryons, are analytical functions of q^2 ; they are closely related to the helicity amplitudes. Due to the crossing symmetry of the respective amplitudes the space-like and time-like regions are connected by dispersion relations. The results obtained for various baryon transitions in the space-like region reveal contributions from a quark core and a meson-cloud, being an important feature at small q^2 [9, 10]. The time-like kinematic domain can be addressed via the Dalitz decay of baryons $R \rightarrow Ne^+e^-$, which probe electromagnetic transitions in the $q^2 = M_{e^+e^-}^2$ interval $[4m_e^2, (M_R - M_N)^2]$. Here $M_{e^+e^-}$ is the dielectron invariant mass and m_e , M_R and M_N are the electron, resonance and nucleon masses, respectively. According to Vector Meson Dominance (VMD) models, light vector mesons ($VM = \rho$ and ω) should play an important role in these transitions. A strong enhancement of eTFF as a function of $M_{e^+e^-}$ approaching VM poles is expected. Indeed, such effects have been observed in meson Dalitz decays, [11–14] but confirmation is lacking for baryons.

The interest on virtual photon coupling to baryons is also driven by the quest for ρ meson in-medium modification, extensively investigated in heavy-ion collisions by means of dilepton spectroscopy (for a review, see [15]). In the context of VMD, the observed strong broadening of the ρ spectral function is explained mainly by ρ -baryon resonance interactions [16], with a major contribution of $N(1520)$ in the second resonance region [17]. However, the mechanism of the coupling is not precisely known.

As first pointed out in [18], the VMD model assuming that coupling proceeds only via ρ strongly overestimates $R \rightarrow N\gamma$ branching ratios and the version of Kroll and Zumino [19] with a superposition of direct photon and ρ meson coupling. It allows to take into account the apparent non-universality of hadron couplings to conserved currents [20, 21] and to fix separately the ρN and γN branching ratios. Consequently, in calculations of the in-medium ρ spectral function of [16] a two-component scheme was applied.

Dedicated microscopic calculations for the $\pi^-p \rightarrow n e^+e^-$ [22, 23] reaction were performed using effective Lagrangian models and the VMD described above. Covariant quark models [24, 25], describing the coupling of the photon to the constituent quark core and to the meson cloud, have been recently extended to the time-like region. The results reveal the dominant role of the latter, with the ρ meson saturating the transition. Effective field, dispersion theory, Dyson-Schwinger or lattice QCD approaches also offer promising perspectives for the calculations of eTFF of baryons [26–30].

After the very first determination of the $\Delta(1232)$ Dalitz decay branching ratio [31] and investigations of higher lying resonances [32, 33] using $p + p$ reactions, the HADES collaboration started new measurements in the second resonance region, using the GSI pion beam facility [34, 35]. As baryon resonances can be excited in pion induced reactions with a fixed mass in the s -channel, they are indeed ideally suited for baryon Dalitz decay studies and offer a unique access to the baryon time-like electromagnetic structure, via the measurement of e^+e^- invariant masses and angular distributions. We are using analysis and simulation inputs presented in detail in [36], where results for the inclusive e^+e^- production are discussed. In this letter, we present measurements of the quasi-free $\pi^-p \rightarrow n e^+e^-$ reactions at a center-of-mass energy $\sqrt{s_{\pi p}} = 1.49 \text{ GeV}/c^2$ using a CH_2 target. Data are compared with predictions of the covariant quark [24, 25] and two-component VDM [23] models.

Experiment. The experiment was performed using a secondary pion beam with central momentum of $0.685 \text{ GeV}/c$ (momentum spread of $\pm 1.7\%$ and incident flux of 10^5 pions/s [34]). Polyethylene (CH_2) and carbon (C) targets were used in separate runs [36]. HADES [37] consists of six identical sectors covering polar angles between 18° and 85° with respect to the beam axis. The information provided by the hadron blind RICH detec-

tor, the tracking and time-of-flight systems was used to reconstruct the four-momentum vectors of the e^+ and e^- [37, 38]. Details about track selection cuts, combinatorial background (CB) subtraction, efficiency corrections as well as normalisation of the measured yields can be found in [36]. For the exclusive channels presented in this analysis, the signal to CB ratio is larger than 50, except for $M_{e^+e^-} \in [100, 140]$ MeV/ c^2 , where values close to unity are reached due to double conversion π^0 decays.

Simulations. As explained in detail in [36], three main sources of e^+e^- pairs are expected to contribute in the energy range of our experiment and were accordingly implemented in simulations: (i) π^0 Dalitz decay $\pi^0 \rightarrow \gamma e^+e^-$, (ii) η Dalitz decay $\eta \rightarrow \gamma e^+e^-$ and (iii) exclusive $\pi^-p \rightarrow n e^+e^-$ reaction. Interactions with carbon nuclei were treated using a quasi-free participant spectator model with a cross section ratio $\sigma_C/\sigma_p = 2.9$ consistent with the measured yields on the polyethylene and carbon targets. The comparison to the results of the inclusive channels allowed to validate the description of the π^0 and η sources.

For the exclusive $\pi^-p \rightarrow n e^+e^-$ reaction channel, isolated as described below, a ‘‘QED reference’’ was first calculated using the cross section of the $\pi^-p \leftrightarrow \gamma n$ reaction. The respective dielectron production was obtained as a non-coherent sum of the Dalitz decays of N(1535) and N(1520) resonances with mass dependent partial decay widths for point-like particles (for details, see sec. IV.A of [36]).

To estimate the effect of the unknown $M_{e^+e^-}$ dependent eTFF, a data-driven VMD approach was used assuming ρ dominance. The ρ contribution was extracted in the Partial Wave Analysis (PWA) of the $\pi^-p \rightarrow n \pi^+\pi^-$ reaction measured in the same experiment [35]. In VMD models, the partial width $\Gamma_{e^+e^-}(M)$ for the decay of the ρ meson into an e^+e^- pair derives from the choice of the Lagrangian for the $\gamma - \rho$ coupling [20]. We have used the two-component VMD [19] (denoted as VMD1 in [20]) with the ρ coupling vanishing at $M_{e^+e^-} = 0$: $\Gamma(M_{e^+e^-}) = \Gamma_\rho M_{e^+e^-} / M_\rho$, where Γ_ρ is the partial decay width at the Breit-Wigner mass M_ρ , entering ρ spectral function:

$$\mathcal{A}(M) = \frac{M^2 \Gamma_{\text{tot}}(M)}{(M_\rho^2 - M^2)^2 + M^2 \Gamma_{\text{tot}}^2(M)}. \quad (1)$$

The total ρ decay width $\Gamma_{\text{tot}}(M)$ includes a parametrization of the $\rho \rightarrow \pi\pi$ decay consistent with the PWA calculations (see [36] for details). The total dielectron yield is obtained as a coherent sum of the photon (‘‘QED reference’’) and the ρ meson contributions, derived as described above. The phase between the two contributions was considered as a free parameter.

In an alternative approach, an eTFF model is implemented, based on the recently developed covariant quark model for the N-N(1520) [24] and N-N(1535) [25] transitions. The differential Dalitz decay width of $3/2^-$ or

$1/2^-$ baryons depends on the eTFF via the expression

$$\frac{1}{\Gamma^{N^* \rightarrow N\gamma}} \frac{d\Gamma^{N^* \rightarrow Ne^+e^-}}{dM_{e^+e^-}} = \frac{2\alpha}{3\pi M_{e^+e^-}} \frac{\sigma_\pm^3 \sigma_-}{m_\pm^3 m_-} \frac{|G_T(q^2)|^2}{|G_T(0)|^2}, \quad (2)$$

where $m_\pm = M_R \pm M_N$ and $\sigma_\pm^2 = m_\pm^2 - q^2$. α is the fine-structure constant, $\Gamma^{N^* \rightarrow N\gamma}$ is the radiative decay width and $|G_T(q^2)|^2$ is a combination of the squared moduli of the electric, magnetic and Coulomb form factors, as given in [36]. In our simulation, we used the mass dependence of $|G_T(q^2)|^2$ from the model of [24, 39], where it is governed by the pion form factor and is similar for N(1520) and N(1535). The overall normalisation of the calculation was fixed to ensure consistency of the dielectron yield with the $\pi^-p \rightarrow n\gamma$ cross section.

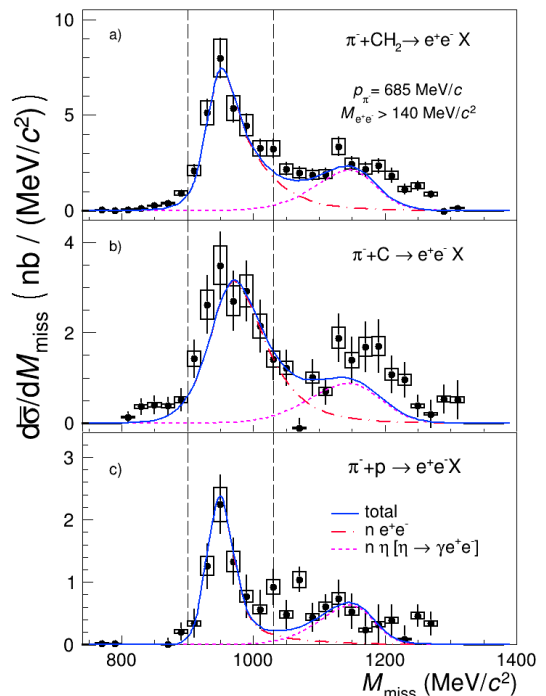


FIG. 1. Distribution of the missing mass M_{miss} calculated *w.r.t.* the π^-p system for a fixed pion beam momentum of 0.685 GeV/ c for events with e^+e^- invariant mass larger than 140 MeV/ c^2 . Data (symbols with error bars) for $\pi^+ + \text{CH}_2$ (a), $\pi^+ + \text{C}$ (b) and $\pi^+ + p$ (c) are displayed after efficiency corrections. Simulated distributions (curves) after full reconstruction are shown for the $\pi^-p \rightarrow n e^+e^-$ channel using the eTFF model (dotted-dashed red), η Dalitz decay (dashed magenta) and the total (blue). The vertical dashed lines indicate the missing mass window used to select events of the $\pi^-p \rightarrow n e^+e^-$ reaction.

Exclusive channel selection. For $M_{e^+e^-}$ larger than the π^0 mass, a cut on the missing mass $M_{\text{miss}} = \sqrt{(P_{\text{in}} - P_{\text{out}})^2}$, where $P_{\text{in}} = p_\pi + p_p$ and $P_{\text{out}} = p_{e^+} + p_{e^-}$, are used to select the exclusive $\pi^-p \rightarrow n e^+e^-$ process (Fig. 1). P_{in} is calculated for a fixed pion mo-

mentum of 0.685 GeV/c incident on a free proton at rest. The cross sections integrated over the HADES acceptance (denoted by $\bar{\sigma}$ throughout this letter) for the CH₂ (Fig. 1a) and C (Fig. 1b) targets have been subtracted to determine the distribution for π^- p interactions (Fig. 1c). The three distributions show two similar structures, which are well reproduced by the simulations: a peak around the neutron mass, which can be attributed to the exclusive π^- p \rightarrow n e⁺e⁻ reaction, either on a free proton or a bound proton in the carbon nuclei and a broader structure, primarily due to the η Dalitz decay, as validated in [40]. The width of the neutron peak obtained for the free π^- p \rightarrow n e⁺e⁻ reaction is mainly due to the detector resolution, with only a minor impact of the pion beam momentum spread, while, for the carbon target, it mainly results from the nucleon momentum distributions. It can also be observed that the eTFF model, which is used here to describe the π^- p \rightarrow n e⁺e⁻ process, provides a good description of the yields. The second structure is well reproduced by the simulation of the η Dalitz decay, although contributions from the Bremsstrahlung process, of the type $\pi^-N \rightarrow \pi N e^+e^-$, might be responsible for the missing yield $M_{\text{miss}} > M_N + m_\pi$. These results are fully consistent with the analysis of the inclusive e⁺e⁻ production [36]. Due to the low statistics recorded on the carbon target (Fig. 1b), the precision obtained separately for π^- p and π^- C interactions is limited and does not allow for an accurate study of the corresponding distributions as a function of invariant mass or angles. One should stress, however, that a very good description of the neutron peak in the π^- C case justifies the assumption about the quasi-free character of the reaction. Therefore, the focus of this analysis is on the polyethylene target measurements. The exclusive quasi-free π^- p \rightarrow n e⁺e⁻ channel is selected henceforth by applying the missing mass selection $900 \text{ MeV}/c^2 < M_{\text{miss}} < 1030 \text{ MeV}/c^2$.

Invariant masses. As shown in Fig. 2a), the π^0 Dalitz decay is not fully suppressed by this missing mass cut. This contribution is, however, well described by the simulation, which is therefore used to subtract its yield. The further analysis is based on 1280 e⁺e⁻ pairs with $M_{e^+e^-} > 100 \text{ MeV}/c^2$, which remain after this subtraction. Acceptance correction factors are deduced in each 20 MeV/c² wide invariant mass bin, using the simulation with the eTFF model, which lead to an average correction factor of about 5.9 with a smooth invariant mass dependence. Due to the model dependence of this correction, the corrected yields are affected by a systematic error of 5 %. The effect of the missing mass cut, which is not corrected for, amounts to a loss of about 20 %, according to the simulations. To determine cross sections for the quasi-free reaction π^- p \rightarrow n e⁺e⁻, the number of effective protons $Z_{\text{eff}} + 2 = 4.9 \pm 0.5$ [36], contributing to the $\pi^- + \text{CH}_2$ reaction, has been taken into account. The resulting invariant mass spectrum is compared to the result of our simulations in Fig. 2b). Below 200 MeV/c², the

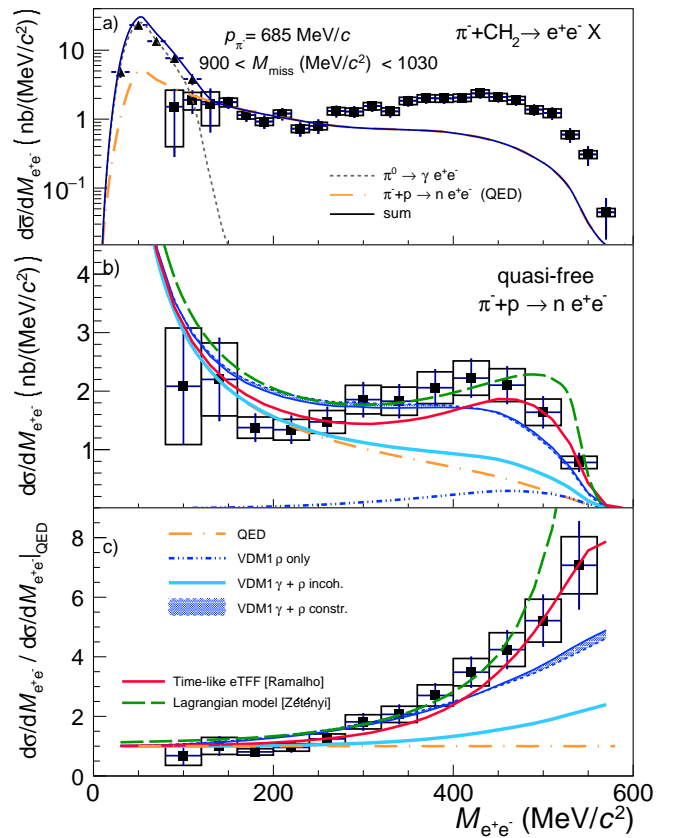


FIG. 2. (a) $d\bar{\sigma}/dM_{e^+e^-}$ for the $\pi^- + \text{CH}_2$ reaction integrated in the HADES acceptance over the missing mass range [900-1030] MeV/c². Full triangles: total yields, full squares: after subtraction of the π^0 Dalitz decay contribution ($\pi^0[\gamma e^+e^-]$). The curves display the simulations for point-like baryon Dalitz decay (“QED reference”, orange dashed-dotted curve), π^0 Dalitz decay (black dotted curve) and the sum (black solid curve). (b) $d\sigma/dM_{e^+e^-}$ for the quasi-free π^- p \rightarrow n e⁺e⁻ reaction integrated over the missing mass range [900-1030] MeV/c² after normalisation by the number of effective protons and acceptance corrections. Orange dashed-dotted curve: QED reference ($d\sigma/dM_{e^+e^-}|_{\text{QED}}$), blue thick (cyan thick) curve: two-component VMD model with constructive (incoherent) sum of ρ and γ contributions, dashed-dot-dot-dashed blue curve: ρ contribution to VMD1. Calculations using the time-like form-factor model (red solid curve) and the Lagrangian model (green long dashed curve) are also shown. (c) Ratios $(d\sigma/dM_{e^+e^-})/(d\sigma/dM_{e^+e^-}|_{\text{QED}})$. The same marker and curve styles apply as in panel (b). Symbols with vertical and horizontal bars show the data with total and systematic point-to-point errors, respectively, and curves display simulations with absolute normalisation in all panels.

experimental cross section is in fair agreement with the QED reference. However, at larger invariant masses, an excess of up to a factor 7 is observed, pointing to a strong effect of the eTFF. To demonstrate this effect more directly, the ratios of data and simulations to the QED reference are displayed in Fig. 2c), which can be considered a measure of the effective eTFF in the π^- p \rightarrow n e⁺e⁻

reaction.

Comparison to models. The various eTFF models mentioned above can be confronted with data. First, it is interesting to check the model based on the ρ contributions from the PWA analysis. As shown in Fig. 2b), the yields above $300 \text{ MeV}/c^2$ depend on the interference between the ρ and γ amplitudes. An incoherent sum of the two contributions (thick cyan curve) significantly underestimates the data, but a better description of the e^+e^- invariant mass spectrum can be obtained using a maximum constructive interference (blue colored area). As shown in detail in [36], the effect of the Fermi motion on the simulated invariant mass distribution for the quasi-free reaction is very small.

Our data are also compared to the microscopic calculation of [23] based on an effective Lagrangian approach, taking into account various resonant and non-resonant amplitudes in a coherent way. The calculation uses the $N^*N\rho$ couplings derived from the PWA [35]. A salient feature of this model is the application of the two-component VMD model to all baryon-photon couplings. Choosing a relative phase of 90° between the resonant γ and ρ amplitudes, a good description of the e^+e^- production is achieved, as shown by the green long dashed curve in Figs. 2b) and c). Simulations based on the eTFF model [24, 25] for these resonances also give a satisfactory description of the data, which demonstrates that the meson cloud contribution, driven by the pion electromagnetic form factor, plays indeed a dominant role.

The measured e^+e^- cross section for $M_{e^+e^-} \approx 500 \text{ MeV}/c^2$ is more than two orders of magnitude larger than the calculations of [22], which were based on a very low off-shell ρ cross section and strong destructive interferences with off-shell ω production. The calculations of [41], which were performed for $\sqrt{s_{\pi p}}$ larger than 1.6 GeV , also predicted large negative interferences between ρ and ω , though with a larger ρ yield.

The ‘‘QED reference’’ model was used to extrapolate the experimental differential cross section at small invariant masses $M_{e^+e^-} < 100 \text{ MeV}/c^2$. In this way, a total cross section for the free $\pi^-p \rightarrow n e^+e^-$ reaction of $\sigma = (2.97 \pm 0.07^{\text{data}} \pm 0.21^{\text{acc}} \pm 0.31^{\text{Zeff}}) \mu\text{b}$ can be deduced, where the errors are due to uncertainties of the measurement, the acceptance correction and the effective number of protons, respectively. The ratio of the integrated experimental and ‘‘QED reference’’ cross sections, which can be attributed to an effective eTFF, amounts to 1.35 ± 0.03 (data) ± 0.02 (acceptance).

Angular distributions. Further information on the nature of the time-like electromagnetic transitions in the $\pi^-p \rightarrow n e^+e^-$ reaction can be obtained from the angular distributions. A convenient parameterization of the differential cross sections $d^4\sigma/d\Theta_{\gamma^*}dM_{e^+e^-}d\cos\Theta d\phi \propto |A|^2$ is provided by the density matrix formalism [23, 42, 43] with the relevant dependencies of the mod-squared

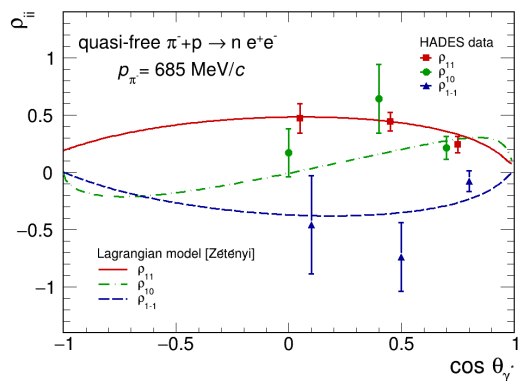


FIG. 3. Results of the analysis of the e^+ and e^- angular distributions in the quasi-free $\pi^-p \rightarrow n e^+e^-$ reaction at $\sqrt{s_{\pi p}} = 1.49 \text{ GeV}$. Spin density matrix elements ρ_{ij} : ρ_{11} (red symbols), ρ_{10} (green symbols) and ρ_{1-1} (blue symbols) extracted for e^+e^- events with $M_{e^+e^-} > 300 \text{ MeV}/c^2$, are shown in 3 bins of the cosine of the virtual photon angle θ_{γ^*} ($[-0.2, 0.3]$, $[0.3, 0.6]$, $[0.6, 0.95]$) compared to the predictions of the model [23] for ρ_{11} (full curve), ρ_{10} (dash-dotted curve) and ρ_{1-1} (dashed curve).

amplitude $|A|^2$ at given value of $M_{e^+e^-}$ and polar angle (Θ_{γ^*}) of the virtual photon in the center-of-mass frame:

$$|A|^2 \propto 8k^2 [1 - \rho_{11} + (3\rho_{11} - 1) \cos^2 \Theta + \sqrt{2} \text{Re} \rho_{10} \sin 2\Theta \cos \phi + \text{Re} \rho_{1-1} \sin^2 \Theta \cos 2\phi]. \quad (3)$$

Here, k , Θ and ϕ denote the momentum, the polar and azimuthal angles of the electron in the virtual photon reference frame, respectively, and $\rho_{11,10,1-1}$ are the three independent density matrix coefficients, which, for a given transition are related to the corresponding eTFF [44]. A method to extract these quantities from a fit to experimental data has been developed taking into account acceptance and detector inefficiency effects [43, 45, 46]. Although the statistics of the measurement is limited, the coefficients can be extracted as a function of the γ^* emission angle in the center-of-mass for $M_{e^+e^-} > 300 \text{ MeV}/c^2$, as shown in Fig. 3. The significant deviations of ρ_{11} from 0.5 and of ρ_{10} from 0 observed for the last angular bin clearly demonstrate the contributions of virtual photons with longitudinal polarization, in contrast to real photons. The angular dependence of the coefficients indicate important contributions of spins larger than $1/2$, in agreement with the dominance of the $N(1520)$ resonance in the ρ production, which was found in the PWA of the two-pion production [35]. The results are also compared to the predictions of the Lagrangian model [23] for an invariant mass $M_{e^+e^-} = 400 \text{ MeV}/c^2$ and a phase $\Phi = 90^\circ$ between the photon and ρ contribution, to be consistent with the comparison of invariant mass distributions (Fig. 2). The main trend of the data is accounted for, which indicates a realistic description of the virtual

photon polarization and a dominant $J=3/2$ contribution in the model.

Summary. In summary, e^+e^- production has been measured in pion induced reactions at a momentum of $0.685 \text{ GeV}/c$, opening a window on the time-like electromagnetic structure of baryon transitions in the second resonance region. The data for the quasi-free $\pi^-p \rightarrow n e^+e^-$ reaction are consistent with the $\pi^-p \rightarrow \gamma n$ results for invariant masses below $250 \text{ MeV}/c^2$, while an excess by up to a factor 7 is observed for larger invariant masses. The effective mass dependent eTFF was derived from data and found to be in good agreement with the predictions of a covariant eTFF model of $N-N(1520)$ and $N-N(1535)$ transitions [25, 39]. The enhancement is explained by a strong meson cloud contribution, in line with conclusions derived from electron scattering experiments in the space-like region. The two-component approach, based on the coherent sum of a direct photon and a ρ amplitude derived from the VMD1 Lagrangian [20], allows for a good description of our data over the full e^+e^- invariant mass range. Based on the existing PWA solution for the two-pion production at the same energy [35], this approach provides a fully consistent description of electromagnetic and hadronic channels in the π^-p reaction. For the first time, the results quantify the important role of the ρ in baryon resonance transitions. The nature of the transition, with a dominant contribution from $N-N(1520)$, is corroborated by the extraction of the spin density matrix elements. A Lagrangian model based on the same VMD approach for each resonant and non-resonant contribution provides a fair description of the invariant mass distribution and the spin density matrix elements.

These pioneering results constitute a new insight into the nature of baryon-virtual photon coupling in the time-like region. Our data clearly demonstrate the two-component character of the time-like electromagnetic baryon transition, with the coupling via vector mesons taking over the direct coupling with increasing invariant mass. A successful description of the data by models assuming on one side the dominance of N^* resonances and non-resonant contributions on the other, might suggest the universal character of the coupling based on this scheme. However, the present results do not yet allow to separate non-resonant and resonant contributions. Future experiments aiming for high statistics scans of the third and second resonance regions combined with measurements of electron angular distributions are planned with HADES. The results call also for the development of phenomenological tools to extract contributions from magnetic, electric and Coulomb eTFF from invariant mass and angular distributions.

We appreciated the theoretical tools provided by A. Sarantsev, G. Ramalho and M. T. Peña. We are very grateful for interesting discussions on theoretical aspects with K. Gallmeister and U. Mosel. We acknowledge

support from SIP JUC Cracow, Cracow (Poland), National Science Center, 2016/23/P/ST2/040 POLONEZ, 2017/25/N/ST2/00580, 2017/26/M/ST2/00600; TU Darmstadt, Darmstadt (Germany), DFG GRK 2128, DFG CRC-TR 211, BMBF:05P18RDFC1, HFHF, ELEMENTS:500/10.006, VH-NG-823, GSI F&E, ExtreMe Matter Institute EMMI at GSI Darmstadt; Goethe-University, Frankfurt (Germany), BMBF:05P12RFGHJ, GSIF&E, HIC for FAIR (LOEWE), ExtreMe Matter Institute EMMI at GSI Darmstadt; TU München, Garching (Germany), MLL München, DFG EClust 153, GSI TMLRG1316F, BmBF 05P15WOFCA, SFB 1258, DFG FAB898/2-2; JLU Giessen, Giessen (Germany), BMBF:05P12RGGHM; IJCLab Orsay, Orsay (France), CNRS/IN2P3, P2IO Labex, France; NPI CAS, Rez, Rez (Czech Republic), MSMT LM2018112, LTT17003, MSMT OP VVV CZ.02.1.01/0.0/0.0/18 046/0016066.

We acknowledge the contribution from the following colleagues: A. Belyaev, O. Fateev, M. Golubeva, F. Guber, A. Ierusalimov, A. Ivashkin, A. Kurepin, A. Kurilkin, P. Kurilkin, V. Ladygin, A. Lebedev, M. Mamaev, S. Morozov, O. Petukhov, A. Reshetin, A. Sadovsky, A. Shabanov, and A. Taranenko.

-
- [1] I. G. Aznauryan *et al.* (CLAS), Electroexcitation of nucleon resonances from CLAS data on single pion electroproduction, *Phys. Rev.* **C80**, 055203 (2009), arXiv:0909.2349 [nucl-ex].
 - [2] R. Thompson *et al.* (CLAS), The $ep \rightarrow e'p\eta$ reaction at and above the $S(11)(1535)$ baryon resonance, *Phys. Rev. Lett.* **86**, 1702 (2001), arXiv:hep-ex/0011029 [hep-ex].
 - [3] I. Aznauryan *et al.*, Studies of Nucleon Resonance Structure in Exclusive Meson Electroproduction, *Int. J. Mod. Phys.* **E22**, 1330015 (2013), arXiv:1212.4891 [nucl-th].
 - [4] V. I. Mokeev *et al.*, New Results from the Studies of the $N(1440)1/2^+$, $N(1520)3/2^-$, and $\Delta(1620)1/2^-$ Resonances in Exclusive $ep \rightarrow e'p'\pi^+\pi^-$ Electroproduction with the CLAS Detector, *Phys. Rev.* **C93**, 025206 (2016), arXiv:1509.05460 [nucl-ex].
 - [5] E. L. Isupov *et al.* (CLAS), Measurements of $ep \rightarrow e'\pi^+\pi^-p'$ Cross Sections with CLAS at $1.40 \text{ GeV} < W < 2.0 \text{ GeV}$ and $2.0 \text{ GeV}^2 < Q^2 < 5.0 \text{ GeV}^2$, *Phys. Rev.* **C96**, 025209 (2017), arXiv:1705.01901 [nucl-ex].
 - [6] S. Bereznev *et al.*, The Measurement of the Pion and Nucleon Form-Factors in the Region of the Timelike 4-Momentum Transfers from 1.5 to 3.0 fm^{-2} , *Sov. J. Nucl. Phys.* **24**, 591 (1976).
 - [7] C. M. Hoffman, J. S. Frank, R. E. Mischke, D. C. Moir, J. S. Sarracino, P. A. Thompson, and M. A. Scharidt, A measurement of $\pi^-p \rightarrow ne^+e^-$ at $300 \text{ MeV}/c$ and a search for scalar and vector bosons heavier than the π^0 , *Phys. Rev. D* **28**, 660 (1983).
 - [8] A. P. Ierusalimov and G. I. Lykasov, Dielectron Production in Pion-Nucleon Reactions at Intermediate Energies, *Phys. Part. Nucl. Lett.* **15**, 457 (2018).
 - [9] B. Julia-Diaz, T. S. H. Lee, A. Matsuyama, T. Sato,

- and L. C. Smith, Dynamical coupled-channels effects on pion photoproduction, *Phys. Rev.* **C77**, 045205 (2008), arXiv:0712.2283 [nucl-th].
- [10] I. G. Aznauryan and V. Burkert, Electroexcitation of nucleon resonances of the $[70, 1^-]$ multiplet in a light-front relativistic quark model, *Phys. Rev.* **C95**, 065207 (2017), arXiv:1703.01751 [nucl-th].
- [11] H. Berghauer *et al.*, Determination of the eta-transition form factor in the gamma $p \rightarrow p\eta \rightarrow p\gamma e^+ e^-$ reaction, *Phys. Lett.* **B701**, 562 (2011).
- [12] P. Aguar-Bartolome *et al.* (A2), New determination of the η transition form factor in the Dalitz decay $\eta \rightarrow e^+e^-\gamma$ with the Crystal Ball/TAPS detectors at the Mainz Microtron, *Phys. Rev.* **C89**, 044608 (2014), arXiv:1309.5648 [hep-ex].
- [13] R. Arnaldi *et al.* (NA60), Precision study of the $\eta \rightarrow \mu^+\mu^-\gamma$ and $\omega \rightarrow \mu^+\mu^-\pi^0$ electromagnetic transition form-factors and of the $\rho \rightarrow \mu^+\mu^-$ line shape in NA60, *Phys. Lett.* **B757**, 437 (2016), arXiv:1608.07898 [hep-ex].
- [14] P. Adlarson *et al.*, Measurement of the $\omega \rightarrow \pi^0 e^+e^-$ and $\eta \rightarrow e^+e^-\gamma$ Dalitz decays with the A2 setup at MAMI, *Phys. Rev.* **C95**, 035208 (2017), arXiv:1609.04503 [hep-ex].
- [15] P. Salabura and J. Stroth, Dilepton radiation from strongly interacting systems, *Prog. Part. Nucl. Phys.* **120**, 103869 (2021), arXiv:2005.14589 [nucl-ex].
- [16] R. Rapp and J. Wambach, Chiral symmetry restoration and dileptons in relativistic heavy ion collisions, *Adv. Nucl. Phys.* **25**, 1 (2000), arXiv:hep-ph/9909229 [hep-ph].
- [17] W. Peters, M. Post, H. Lenske, S. Leupold, and U. Mosel, The Spectral function of the rho meson in nuclear matter, *Nucl. Phys. A* **632**, 109 (1998), arXiv:nucl-th/9708004.
- [18] B. Friman, Meson nucleon scattering and vector mesons in nuclear matter, *Acta Phys. Polon. B* **29**, 3195 (1998), arXiv:nucl-th/9808071.
- [19] N. M. Kroll, T. D. Lee, and B. Zumino, Neutral Vector Mesons and the Hadronic Electromagnetic Current, *Phys. Rev.* **157**, 1376 (1967).
- [20] H. B. O'Connell, B. C. Pearce, A. W. Thomas, and A. G. Williams, $\rho - \omega$ mixing, vector meson dominance and the pion form-factor, *Prog. Part. Nucl. Phys.* **39**, 201 (1997), arXiv:hep-ph/9501251 [hep-ph].
- [21] G. E. Brown, M. Rho, and W. Weise, Phenomenological Delineation of the Quark - Gluon Structure From Nucleon Electromagnetic Form-factors, *Nucl. Phys. A* **454**, 669 (1986).
- [22] M. Lutz, B. Friman, and M. Soyeur, Quantum interference of rho0 and omega-mesons in the $\pi N \rightarrow e^+e^-N$ reaction, *Nucl. Phys. A* **713**, 97 (2003).
- [23] M. Zétényi, D. Nitt, M. Buballa, and T. Galatyuk, Role of baryon resonances in the $\pi-p \rightarrow ne+e-$ reaction within an effective-Lagrangian model, *Phys. Rev. C* **104**, 015201 (2021), arXiv:2012.07546 [nucl-th].
- [24] G. Ramalho and M. T. Peña, $\gamma^*N \rightarrow N(1520)$ form factors in the timelike regime, *Phys. Rev.* **D95**, 014003 (2017), arXiv:1610.08788 [nucl-th].
- [25] G. Ramalho and M. T. Peña, Covariant model for the Dalitz decay of the $N(1535)$ resonance, *Phys. Rev.* **D101**, 114008 (2020), arXiv:2003.04850 [hep-ph].
- [26] S. Leupold and C. Terschlusen, Towards an effective field theory for vector mesons, *Proceedings, 50th International Winter Meeting on Nuclear Physics (Bormio 2012): Bormio, Italy, January 23-27, 2012*, PoS **BORMIO2012**, 024 (2012), arXiv:1206.2253 [hep-ph].
- [27] An Di, proc. of MESON 2023, to be published.
- [28] C. Granados, S. Leupold, and E. Perotti, The electromagnetic Sigma-to-Lambda hyperon transition form factors at low energies, *Eur. Phys. J. A* **53**, 117 (2017), arXiv:1701.09130 [hep-ph].
- [29] G. Eichmann *et al.*, Baryons as relativistic three-quark bound states, *Prog. Part. Nucl. Phys.* **91**, 1 (2016), arXiv:1606.09602 [hep-ph].
- [30] A. S. Miramontes, H. Sanchis Alepuz, and R. Alkofer, Elucidating the effect of intermediate resonances in the quark interaction kernel on the timelike electromagnetic pion form factor, *Phys. Rev. D* **103**, 116006 (2021).
- [31] J. Adamczewski-Musch *et al.* (HADES), $\Delta(1232)$ Dalitz decay in proton-proton collisions at $T=1.25$ GeV measured with HADES at GSI, *Phys. Rev.* **C95**, 065205 (2017), arXiv:1703.07840 [nucl-ex].
- [32] G. Agakishiev *et al.* (HADES), Inclusive dielectron spectra in p+p collisions at 3.5 GeV, *Eur. Phys. J.* **A48**, 64 (2012), arXiv:1112.3607 [nucl-ex].
- [33] G. Agakishiev *et al.* (HADES), Inclusive dielectron production in proton-proton collisions at 2.2 GeV beam energy, *Phys. Rev.* **C85**, 054005 (2012), arXiv:1203.2549 [nucl-ex].
- [34] J. Adamczewski-Musch *et al.* (HADES), A facility for pion-induced nuclear reaction studies with HADES, *Eur. Phys. J.* **A53**, 188 (2017).
- [35] J. Adamczewski-Musch *et al.* (HADES), Two-Pion production in the second resonance region in π^-p collisions with HADES, *Phys. Rev.* **C102**, 024001 (2020), arXiv:2004.08265 [nucl-ex].
- [36] R. Abou Yassine *et al.*, Inclusive e^+e^- production from quasi-free reactions in the second resonance region, submitted to PRC (2023).
- [37] G. Agakishiev *et al.* (HADES), The High-Acceptance Dielectron Spectrometer HADES, *Eur. Phys. J.* **A41**, 243 (2009), arXiv:0902.3478 [nucl-ex].
- [38] P. Sellheim, *Reconstruction of the low-mass dielectron signal in 1.23A GeV Au+Au collisions*, PhD-thesis, University of Frankfurt, 2017.
- [39] G. Ramalho *et al.*, Role of the pion electromagnetic form factor in the $\Delta(1232) \rightarrow \gamma^*N$ timelike transition, *Phys. Rev.* **D93**, 033004 (2016), arXiv:1512.03764 [hep-ph].
- [40] K. Gallmeister, U. Mosel, and L. von Smekal, Dilepton decay of low-mass ρ mesons, *Phys. Rev. C* **106**, 064910 (2022).
- [41] A. I. Titov and B. Kämpfer, Isoscalar-Isovector Interferences in $\pi N \rightarrow Ne^+e^-$ Reactions as a Probe of Baryon Resonance Dynamics, *Eur. Phys. J.* **A12**, 217 (2001), arXiv:nucl-th/0108019.
- [42] E. Speranza, M. Zetenyi, and B. Friman, Polarization and dilepton anisotropy in pion-nucleon collisions, *Phys. Lett.* **B764**, 282 (2017), arXiv:1605.04954 [hep-ph].
- [43] A. Sarantsev, private communication.
- [44] M. Zetenyi, Procs. of NSTAR 2022, to be published.
- [45] B. Ramstein (HADES), Studying time-like electromagnetic baryonic transitions with HADES in pion induced reactions, EPJ Web Conf. **241**, 01012 (2020).
- [46] F. Scozzi, *Studying excited states of the nucleon with the HADES detector at GSI*, PhD-thesis, Paris-Saclay and TU Darmstadt universities (2018).